

Spin-Frustrated Trinuclear Cu(II) Clusters with Mixing of $2(S = 1/2)$ and $S = 3/2$ States by Antisymmetric Exchange. 1. Dzialoshinsky–Moriya Exchange Contribution to Zero-Field Splitting of the $S = 3/2$ State

Moisey I. Belinsky*

School of Chemistry, Sackler Faculty of Exact Sciences, Tel-Aviv University,
Tel Aviv, Ramat Aviv 69978, Israel

Received September 12, 2007

The mixing of the spin-frustrated $2(S = 1/2)$ and $S = 3/2$ states by the Dzialoshinsky–Moriya (DM) exchange is considered for the $\text{Cu}_3(\text{II})$ clusters with strong DM exchange coupling. In the antiferromagnetic Cu_3 clusters with strong DM interaction, the $2(S = 1/2)$ – $S = 3/2$ mixing by the in-plane DM exchange (G_x) results in the large positive contribution $2D_{\text{DM}} > 0$ to the axial zero-field splitting (ZFS) $2D$ of the $S = 3/2$ state. The correlations between the ZFS $2D_{\text{DM}}$ of the excited $S = 3/2$ state, sign of G_z and chirality of the ground-state were obtained. In the isosceles Cu_3 clusters, the in-plane DM exchange mixing results in the rhombic magnetic anisotropy of the $S = 3/2$ state. Large distortions result in an inequality of the pair DM parameters, that leads to an additional magnetic anisotropy of the $S = 3/2$ state. In the $\{\text{Cu}_3\}$ nanomagnet, the in-plane DM exchange (G_x, G_y) mixing results in the 58% contribution $2D_{\text{DM}}$ to the observed ZFS $2D$ of the $S = 3/2$ state. The DM exchange and distortions explain the experimental observation that the intensities of the electron paramagnetic resonance (EPR) transitions arising from the $2(S = 1/2)$ group of levels of the $\{\text{Cu}_3\}$ nanomagnet are comparable to each other and are 1 order of magnitude weaker than that of the $S = 3/2$ state. In the ferromagnetic Cu_3 clusters, the in-plane DM exchange mixing of the excited $2(S = 1/2)$ and the ground $S = 3/2$ states results in the large negative DM exchange contribution $2D_{\text{DM}}' < 0$ to the axial ZFS $2D$ of the ground $S = 3/2$ state.

1. Introduction

Polynuclear clusters of metal ions have attracted significant interest as active centers of biological systems,¹ building blocks of molecular magnets,² models for investigation of magnetism at the mesoscopic scale,³ and quantum gates for molecule-based quantum computation.⁴ A large number of

the copper(II) trimers in coordination compounds and biological systems were investigated in detail.^{1c,d,5–23} The isotropic antiferromagnetic (AFM, $J > 0$) exchange interac-

* E-mail: belinski@post.tau.ac.il. Phone: 972-3-640-79-42. Fax: 972-3-640-92.

- (1) (a) Holm, R. H.; Kennepohl, P.; Solomon, E. I. *Chem. Rev.* **1996**, *96*, 2239. (b) Beinert, H.; Holm, R. H.; Münck, E. *Science* **1997**, *277*, 653. (c) Solomon, E. I.; Sandaram, U. H.; Machonkin, T. E. *Chem. Rev.* **1996**, *96*, 2563. (d) Solomon, E. I.; Baldwin, M. J.; Lowery, M. D. *Chem. Rev.* **1992**, *92*, 521.
- (2) *Molecular Magnetism; From Molecular Assemblies to the Devices*; Coronado, E., Delhaes, P., Gatteschi, D., Miller, J. S., Eds.; NATO ASI Series 321; Kluwer: Dordrecht, 1996.
- (3) Kahn, O. *Molecular Magnetism*; VCH: New York, 1993.
- (4) Carretta, S.; Santini, P.; Amoretti, G.; Troiani, F.; Affronte, M. *Phys. Rev. B* **2007**, *76*, 024408.
- (5) (a) Beckett, R.; Colton, R.; Hoskins, B. F.; Martin, R. L.; Vince, D. G. *Aust. J. Chem.* **1969**, *22*, 2527. (b) Butcher, R. J.; O'Connor, C. J.; Sinn, E. *Inorg. Chem.* **1981**, *20*, 537. (c) Griffith, J. S. *Struct. Bonding (Berlin)* **1972**, *10*, 87. (d) Sinn, E. *Coord. Chem. Rev.* **1970**, *5*, 313.

- (6) (a) Tsukerblat, B. S.; Belinsky, M. I. *Magnetochemistry and Radiospectroscopy of Exchange Clusters*; Shtiintsa: Kishinev, USSR, 1983. (b) Tsukerblat, B. S.; Belinsky, M. I.; Fainzilberg, V. E. *Sov. Sci. Rev. B. Chem.* **1987**, *9*, 337.
- (7) (a) Belinsky, M. I.; Tsukerblat, B. S.; Ablov, A. V. *Fiz. Tverd. Tela.* **1974**, *16*, 989; *Sov. Phys. Solid State* **1974**, *16*, 639. (b) Belinsky, M. I.; Tsukerblat, B. S.; Ablov, A. V. *Mol. Phys.* **1974**, *28*, 283. (c) Belinsky, M. I.; Kuyavskaya, B. Ya.; Tsukerblat, B. S.; Ablov, A. V.; Kushkulei, L. M. *Koord. Chem.* **1976**, *2*, 1099.
- (8) (a) Belinsky, M. I.; Tsukerblat, B. S.; Ablov, A. V. *Dokl. Phys. Chem.* **1972**, *207*, 911. (b) Belinsky, M. I.; Tsukerblat, B. S.; Ablov, A. V. *Phys. Status Solidi* **1972**, *51*, K71.
- (9) (a) Tsukerblat, B. S.; Novotortsev, V. M.; Kuyavskaya, B. Ya.; Belinsky, M. I.; Ablov, A. V.; Bazhan, A. N.; Kalinnikov, V. T. *Sov. Phys. JEPT Lett.* **1974**, *19*, 277. (b) Tsukerblat, B. S.; Kuyavskaya, B. Ya.; Belinsky, M. I.; Ablov, A. V.; Novotortsev, V. M.; Kalinnikov, V. T. *Theor. Chim. Acta* **1975**, *38*, 131.
- (10) (a) Belinsky, M. I. *Inorg. Chem.* **2004**, *43*, 739. (b) Shames, A. I.; Belinsky, M. I. *Phys. Status Solidi* **1997**, *203*, 235.
- (11) (a) Banci, L.; Bencini, A.; Gatteschi, D. *Inorg. Chem.* **1983**, *22*, 2681. (b) Banci, L.; Bencini, A.; Dei, A.; Gatteschi, D. *Inorg. Chem.* **1983**, *22*, 4018. (c) Padilla, J.; Gatteschi, D.; Chaudhuri, P. *Inorg. Chim. Acta* **1997**, *260*, 217.

Table 1. Trinuclear Cu₃(II) Clusters with Antisymmetric DM Exchange Coupling

Cu ₃ compound, ref	J_{ij}/cm^{-1}	$ G_z /\text{cm}^{-1}$	G_z/J_{av}
1. [Cu ₃] ^{6,9}	$J_0 > 300$	6	0.020
2. [Cu ₃] ^{11c}	$J_0 > 150$	5.5	0.037
3. {Cu ₃ (μ_3 -O)(N-N) ₃ } complex 1 ¹⁸	$J' = 156.4, J = 191, \delta = 34.6, J_{\text{av}} = 179.5$	27.8	0.155
4. {Cu ₃ (μ_3 -O)(N-N) ₃ } complex 2 ¹⁸	$J' = 153.2, J = 175.4, \delta = 22.2, J_{\text{av}} = 168$	31	0.185
5. [Cu ₃ (μ_3 -OMe)] complex 1 ¹⁹	$J' = 210, J = 186, \delta = 24, J_{\text{av}} = 194$	33	0.170
6. [Cu ₃ (μ_3 -OMe)] complex 2 ¹⁹	$J' = 252, J = 189, \delta = 63, J_{\text{av}} = 210$	47	0.224
7. TrisOH Cu ₃ (II) ²⁰	$J' = 210, \delta = 17.5$	36	0.167
8. (a) μ_3 O Cu ₃ (II), ²¹ (b) μ_3 OH	(a) $J_0 = -109$, FM, (b) $J_0 = -37.8$	40	0.367
9. {Cu ₃ }, $2D_c = 0.046 \text{ cm}^{-1}$ ^{23a}	$J' = 3.14, J = 2.81, \delta = 0.33, J_{\text{av}} = 2.92$	$G_{x,y,z} = 0.37, G = 0.641$	0.127, $G/J_{\text{av}} = 0.220$

tion $H_0 = \sum J_{ij} S_i S_j$ in trigonal clusters ($J_{ij} = J_0$) leads to the spin-frustrated $2(S = 1/2)$ (2E) ground-state and excited $S = 3/2$ (4A_2) states.⁶⁻⁹ The antisymmetric Dzialoshinsky–Moriya (DM)^{24,25} exchange coupling

$$H_{\text{DM}} = \sum G_{ij} [\mathbf{S}_i \times \mathbf{S}_j] \quad (1)$$

results in the zero-field splitting (ZFS) $\Delta_{\text{DM}}^0 = |G_z| \sqrt{3}$ of the $2(S = 1/2)$ state of the Cu₃(II) clusters,⁶ which determines the anisotropy of the electron paramagnetic resonance (EPR)

- (12) Bencini, A.; Gatteschi, D. *EPR of Exchanged-Coupled Systems*; Springer: Berlin, 1990.
- (13) (a) Chandhuri, P.; Karpenshtein, I.; Winter, M.; Bultzlaff, G.; Bill, E.; Trautwein, A. X.; Flörke, U.; Haupt, H.-J. *J. Chem. Soc., Chem. Commun.* **1992**, 321. (b) Colacio, E.; Dominguez-Vera, J. M.; Escuer, A.; Klinga, M.; Kiverkaes, R.; Romerosa, A. *J. Chem. Soc., Dalton Trans.* **1995**, 343. (c) Hulsbergen, F. B.; Hoedt, R. W. H.; Verschoor, G. C.; Reedijk, J.; Spek, L. A. *J. Chem. Soc., Dalton Trans.* **1983**, 539.
- (14) (a) Costes, J.-P.; Dahan, F.; Lanrent, J.-P. *Inorg. Chem.* **1986**, 25, 413. (b) Kwiatkowski, M.; Kwiatkowski, E.; Olechnowicz, A.; Ho, D. M.; Deutsch, E. *Inorg. Chem.* **1988**, 150, 65. (c) Azuma, M.; Odaka, T.; Takano, M.; Vander Griend, D. A.; Poeppelmeier, K. R.; Narumi, Y.; Kindo, K.; Mizuno, Y.; Maekawa, S. *Phys. Rev. B* **2000**, 62, R3588. (d) Angaridis, P. A.; Baran, P.; Boča, Cervantes-Lee, F.; Haase, W.; Mezei, G.; Raptis, R. G.; Werner, R. *Inorg. Chem.* **2002**, 41, 2219. (e) Stamatatos, T. C.; Vlahopoulou, J. C.; Sanakis, Y.; Raptopoulou, C. P.; Psycharis, V.; Boudalis, A. K.; Perlepes, S. P. *Inorg. Chem. Commun.* **2006**, 9, 814.
- (15) (a) Kodera, M.; Tachi, Y.; Kita, T.; Kobushi, H.; Sumi, Y.; Kano, K.; Shiro, M.; Koikawa, M.; Tokii, T.; Ohba, M.; Okawa, H. *Inorg. Chem.* **2000**, 39, 226. (b) Lopes-Sandoval, H.; Contreras, R.; Escuer, A.; Vicente, R.; Bernes, S.; Nöth, H.; Leigh, G. J.; Barba-Berhens, N. *J. Chem. Soc., Dalton Trans.* **2002**, 2648. (c) Spiccia, L.; Graham, B.; Hearn, M. T. W.; Lasarev, G.; Moubarak, B.; Murray, K. S.; Tiekink, E. R. T. *J. Chem. Soc., Dalton Trans.* **1997**, 4089. (d) Nguyen, H.-H.; Shiemke, A. K.; Jacobs, S. J.; Hales, B. J.; Lingstrom, M. E.; Chan, S. I. *J. Biol. Chem.* **1994**, 269, 14995.
- (16) (a) Cage, B.; Cotton, F. A.; Dalal, N. S.; Hillard, E. A.; Rakvin, B.; Ramsey, C. M. *J. Am. Chem. Soc.* **2003**, 125, 5270. (b) Clérac, R.; Cotton, F. A.; Dunbar, K. R.; Hillard, E. A.; Petrukhina, M. A.; Smuckler, B. W. *C.R. Acad. Sci. Paris, Chim./Chem.* **2001**, 4, 315. (c) Stone, M. B.; Fernandez-alonso, F.; Adroja, D. T.; Datal, N. S.; Villagran, D.; Cotton, F. A.; Nagler, S. E. *Phys. Rev. B* **2007**, 75, 214427.
- (17) (a) Cole, J. L.; Clark, P. A.; Solomon, E. I. *J. Am. Chem. Soc.* **1990**, 112, 9534. (b) Lee, S.-K.; DeBeere, G. S.; Antholine, W. E.; Hedman, B.; Hodgson, K. O.; Solomon, E. I. *J. Am. Chem. Soc.* **2002**, 124, 6180.
- (18) (a) Ferrer, S.; Lloret, F.; Bertomeu, I.; Alzuel, G.; Borrás, J.; Garsia-Granda, S.; Gonzalez, M.; Haasnoot, G. *Inorg. Chem.* **2002**, 41, 5821. (b) Ferrer, S.; J.; Haasnoot, G.; Reedijk, J.; Muller, E.; Cindi, M. B.; Lanfranchi, M.; Lanfredi, A. M. M.; Ribas, J. *Inorg. Chem.* **2000**, 39, 1859.
- (19) Liu, X.; Miranda, M. H.; McInnes, T. J. L.; Kilner, C. A.; Harlow, M. A. *Dalton Trans.* **2004**, 59.
- (20) (a) Yoon, J.; Mirica, L. M.; Stack, T. D. P.; Solomon, E. I. *J. Am. Chem. Soc.* **2004**, 126, 12586. (b) Mirica, L. M.; Stack, T. D. P. *Inorg. Chem.* **2005**, 44, 2131.
- (21) (a) Yoon, J.; Solomon, E. I. *Inorg. Chem.* **2005**, 44, 8076. (b) Chapulsky, J.; Neese, F.; Solomon, E. I.; Ryde, U.; Rulisek, L. *Inorg. Chem.* **2006**, 45, 11051. (c) Suh, M. P.; Han, M. Y.; Lee, J. H.; Min, K. S.; Hyeon, C. *J. Am. Chem. Soc.*, **1998**, 120, 3819.

and magnetic characteristics,^{6,7,9,11,18-20} $G_z = (G_{12,Z} + G_{23,Z} + G_{31,Z})/3$, where Z is the trigonal axis. In the isosceles Cu₃ clusters ($J_{13} = J_{23} = J, J_{12} = J'$), the splitting $\Delta_0 = \sqrt{(\delta^2 + 3G_z^2)}$ of the $2(S = 1/2)$ state is determined by the parameters of the DM exchange G_z and distortion $\delta = J' - J$.⁶

The AFM^{6,9,11c,18-20} and ferromagnetic²¹ (FM, $J < 0$) Cu₃ clusters with the DM exchange coupling are represented in Table 1. The magnetic, EPR- and MCD^{20a}-spectroscopic properties of the AFM Cu₃ compounds¹⁸⁻²⁰ were interpreted by taking into account large G_z and δ parameters ($G_z/J_{\text{av}} = 0.155-0.225, \delta = 17.5-63 \text{ cm}^{-1}$,¹⁸⁻²⁰ nos. 3-7 in Table 1). These G_z/J_{av} relations are significantly larger than the Moriya's²⁵ estimate of the DM exchange $G/J \sim \Delta g/g \sim 0.01-0.02$. The microscopic origin of the large DM exchange parameter G_z in trimeric Cu₃ clusters was explained by Solomon et al.^{20a,21a} by the large overlap of the d-functions of the neighboring Cu(II) ions in the ground and excited states due to the geometry of the metal centers. The ground 4A_2 level of the FM Cu₃ clusters²¹ is characterized by the large negative axial ZFS $2D = -5 \text{ cm}^{-1} \{-2.04 \text{ cm}^{-1}\}$ that was explained by the anisotropic exchange^{21a} (no. 8, Table 1). This large ZFS can be related^{21a} to the strong DM coupling ($|G_z| = 42 \text{ cm}^{-1}$) in the excited 2E state.

The other example of the system with the relatively strong DM exchange coupling is the {Cu₃} nanomagnet^{23a} (no. 9, Table 1) with the relation $G_z/J_{\text{av}} = 0.12, G/J_{\text{av}} = 0.22, G = \sqrt{(G_x^2 + G_y^2 + G_z^2)}$. ZFS $2D$ of the $S = 3/2$ state was explained^{23a} by the anisotropic Heisenberg exchange; the anisotropy was determined using $2D$ value.

The ZFS of the $S = 3/2$ state of the Cu₃ clusters is described by the standard ZFS Hamiltonian²⁶ of the trigonal system

$$H_{\text{ZFS}} = D_0[S_z^2 - S(S+1)/3] \quad (2)$$

where D_0 is the axial ZFS parameter. The anisotropic exchange^{33,34} $H_{\text{AN}} = \sum J_n S_{in} S_{jn}$ ($n = x, y, z; J_x = J_y \neq J_z$) was usually considered^{20a,21a,23a} as the physical origin of D_0 .

Recently, the effect of quantum magnetization, owing to the spin-frustrated $2(S = 1/2)$ doublets of the AFM triangular

- (22) Glaser, T.; Neidemeir, M.; Grimme, S.; Bill, E. *Inorg. Chem.* **2004**, 43, 5192.
- (23) (a) Choi, K.-Y.; Matsuda, Y. H.; Nojiri, H.; Kortz, U.; Hussain, F.; Stowe, A. C.; Ramsey, C.; Dalal, N. S. *Phys. Rev. Lett.* **2006**, 96, 107202. (b) Kortz, U.; Nellutla, S.; Stowe, A. C.; Dalal, N. S.; van Tol, J.; Bassil, B. S. *Inorg. Chem.* **2004**, 40, 144.
- (24) Dzyaloshinsky, I. *J. Phys. Chem. Sol.* **1958**, 4, 241.
- (25) (a) Moriya, T. *Phys. Rev. Lett.* **1960**, 4, 228. (b) Moriya, T. *Phys. Rev.* **1960**, 120, 91.
- (26) Abragam, A.; Bleaney, B. *Electron Paramagnetic Resonance of Transition Ions*; Clarendon Press: Oxford, 1970.

clusters, was observed in the $\{\text{Cu}_3\}$ nanomagnet^{23a} as well as the V_3 clusters,²⁷ V_3 trimers of the V_{15} molecular magnet^{28–32} with the crossing of the $S = 3/2$ and $S = 1/2$ levels in high magnetic field. Quantum magnetization in the $\{\text{Cu}_3\}$ ^{23a} and V_3 ²⁷ nanomagnets was described by the $2(S = 1/2) - S = 3/2$ mixing in the levels crossing point due to the G_x and G_y components of the vector DM exchange parameter, lying in the plane of the trimeric cluster.^{23a,27–32}

The ZFS of the ground state (GS) $2(S = 1/2)$ of the Cu_3 clusters with strong Heisenberg exchange is only determined by the value $|G_z|$ of the out-of-plane DM parameter^{6–11c,18–21}. The ZFS of the $S = 3/2$ state is determined by the anisotropic exchange. The sign of G_z , the chirality of GS, and the G_x and G_y DM components do not influence the splitting, magnetic behavior and EPR characteristics of GS and the excited state in these systems. At the same time, in the Cu_3 (and V_3) nanomagnets, the in-plane (G_x, G_y) components of the DM vector and the GS chirality^{23a,27} play the principal role in an explanation of the magnetic behavior at high magnetic fields.^{23a,27–32}

The influence of the mixing of the $2(S = 1/2)$ and $S = 3/2$ states by the in-plane DM exchange on the ZFS, magnetic anisotropy and EPR characteristics of GS and excited-state of the Cu_3 clusters with large DM exchange and distortions parameters was not considered. In the Cu_3 clusters with large δ distortions, the effect of the difference of the pair DM exchange parameters on the magnetic anisotropy was not considered. In this paper, we study the contribution of the $[2(S = 1/2) - S = 3/2]$ mixing by the in-plane DM exchange to the ZFS, magnetic anisotropy and EPR characteristics of the $S = 3/2$ and $2(S = 1/2)$ states as well as the effect of distortions and the difference of the DM exchange parameters on the ground excited states mixing in the Cu_3 clusters with strong DM exchange coupling and large δ distortions. The

conditions of the existence of the in-plane G_x, G_y components of the DM exchange in the Cu_3 clusters and the dependence of the DM exchange parameters on the orientation (tilt) of the local magnetic orbitals are considered in an accompanying paper.³⁵

2. DM Exchange Mixing of the $S = 1/2$ and $S = 3/2$ States in the Trigonal Clusters

The Hamiltonian of the system

$$H = J(\mathbf{s}_1\mathbf{s}_2 + \mathbf{s}_2\mathbf{s}_3 + \mathbf{s}_1\mathbf{s}_3) + \delta\mathbf{s}_1\mathbf{s}_2 + \sum G_{ij}[\mathbf{S}_i \times \mathbf{S}_j] + H_{\text{ZFS}}^0 + \sum \mu_{\text{B}}\mathbf{s}_i\mathbf{g}_i\mathbf{H} \quad (3)$$

describes the isotropic Heisenberg exchange, the DM exchange, ZFS, and Zeeman interaction in distorted Cu_3 clusters. The eigenfunctions of the $S = 1/2$ states are characterized by the intermediate spins $S_{12} = 0$ and 1 and can be expressed using the $|\text{S}_1\text{S}_2\text{S}_3\rangle$ basis functions, $\varphi_0(1/2, -1/2) = 1/\sqrt{2}(|\uparrow\downarrow\downarrow\rangle - |\downarrow\uparrow\downarrow\rangle)$, $\varphi_1(1/2, -1/2) = 1/\sqrt{6}(|\uparrow\downarrow\downarrow\rangle + |\downarrow\uparrow\downarrow\rangle - 2|\downarrow\uparrow\uparrow\rangle)$, $M = -1/2$, up and down arrows represent up and down spins, respectively, for \mathbf{S}_i (eqs S1 and S2 in the Supporting Information). Directions of the pair DM vectors \mathbf{G}_{ij} in the trimer are determined by the symmetry conditions.²⁵ The Z components of the pair vectors are equal and directed along Z perpendicular to the plane of the trigonal Cu_3 triangle, $G_{12,Z} = G_{23,Z} = G_{31,Z} = G_z$. In the trigonal cluster ($\delta = 0$), ZFS splitting $E_{1(2)}^0 = +(-)|G_z|\sqrt{3}/2$ does not depend on the sign of G_z . The trigonal wave functions $\Psi_{1\pm}^0(1/2, m)$ and $\Psi_{2\pm}^0(1/2, m)$ which diagonalize H_{DM}^Z are shown in eq S3 of the Supporting Information. The sign of G_z determines the chirality of the lowest $S = 1/2$ Zeeman state with $M = -1/2$: $\Psi_{1+}^0(-1/2) = 1/\sqrt{2}[\varphi_0(-1/2) + i\varphi_1(-1/2)]$ for $G_z < 0$, $\Psi_{2-}^0(-1/2) = 1/\sqrt{2}[\varphi_0(-1/2) - i\varphi_1(-1/2)]$ for $G_z > 0$ (in magnetic field $H_z > 0$).

The correlations between the components of the pair DM vectors, lying in the plane of the triangle, in the pair coordinate system (X'_{ij}, Y'_{ij}) and in the trigonal cluster coordinate system (X, Y) have the form

$$\begin{aligned} G_{12,X} &= G_{12,X'} = G_x, G_{12,Y} = G_{12,Y'} = G_y, \\ G_{23,X} &= -1/2(G_{23,X'} + \sqrt{3}G_{23,Y'}), \\ G_{23,Y} &= 1/2(\sqrt{3}G_{23,X'} - G_{23,Y'}); \\ G_{31,X} &= -1/2(G_{31,X'} - \sqrt{3}G_{31,Y'}), \\ G_{31,Y} &= -1/2(\sqrt{3}G_{31,X'} + G_{31,Y'}) \end{aligned} \quad (4)$$

$G_{12,K'} = G_{23,K'} = G_{31,K'} = G_k$ in the trigonal system, $k = x, y$. The orientation of the pair $G_{ij,X'}$ ($G_{ij,Y'}$) DM component in the trimer plane is perpendicular (parallel) to the $\text{Cu}_i - \text{Cu}_j$ bond, $\text{X}||\text{X}'_{12}, \text{Y}||\text{Y}'_{12}$ (Figure 1 of ref 35). The conditions of the existence of the in-plane $G_{ij,X'}$ and $G_{ij,Y'}$ components of the pair DM exchange vector parameters are considered in ref 35. The G_x and G_y DM coefficients do not contribute linearly to ZFS $\pm G_z\sqrt{3}/2$ of GS $2(S = 1/2)$ of the trigonal cluster. The DM parameters for the $[\text{Cu}_2(\text{II})\text{Cu}(\text{III})]$ cluster were considered in ref 36.

The mixing of the $S = 3/2$ and $S = 1/2$ states was considered^{23a,27a,28–32} in the DM model with the three

- (27) (a) Yamase, T.; Ishikawa, E.; Fukaya, K.; Nojiri, H.; Taniguchi, T.; Atake, T. *Inorg. Chem.* **2004**, *43*, 8150. (b) Nojiri, H.; Ishikawa, E.; Yamase, T. *Progr. Theor. Phys.* **2005**, *292*, Suppl. No 159.
- (28) (a) Chiorescu, I.; Wernsdorfer, W.; Müller, A.; Miyashita, S.; Barbara, B. *Phys. Rev. B* **2003**, *67*, 020402(R). (b) Nojiri, H.; Taniguchi, T.; Ajiro, Y.; Müller, A.; Barbara, B. *Physica B* **2004**, *216*, 346. (c) Chiorescu, I.; Wernsdorfer, W.; Müller, A.; Bogge, H.; Barbara, B. *Phys. Rev. Lett.* **2000**, *84*, 3454. (d) Chiorescu, I.; Wernsdorfer, W.; Müller, A.; Bogge, H.; Barbara, B. *J. Magn. Magn. Mater.* **2000**, *221*, 103.
- (29) (a) Chaboussant, G.; Ochsenbein, S. T.; Seiber, A.; Güdel, H.-U.; Mutka, H.; Müller, A.; Barbara, B. *Europhys. Lett.* **2004**, *66*, 423. (b) Wernsdorfer, W.; Müller, A.; Maily, D.; Barbara, B. *Europhys. Lett.* **2004**, *66*, 861. (c) Sakon, T.; Koyama, K.; Motokawa, M.; Müller, A.; Barbara, B.; Ajiro, Y. *Progr. Theor. Phys.* **2005**, *302*, Suppl. No 159. (d) Machida, M.; Itaka, T.; Miyashita, S. *J. Phys. Soc. Jpn.* **2005**, *74*, 107. (e) Furukawa, Y.; Nishisaka, Y.; Kumagai, K.-i.; Kögerler, P.; Borsari, F. *Phys. Rev. B* **2007**, *75*, 220402(R).
- (30) Konstantinidis, N. P.; Coffey, D. *Phys. Rev. B* **2002**, *66*, 26.
- (31) (a) De Raedt, H.; Miyashita, S.; Michielsen, K.; Machida, M. *Phys. Rev. B* **2004**, *70*, 064401. (b) De Raedt, H.; Miyashita, S.; Michielsen, K. *Phys. Stat. Sol. B* **2004**, *1241*, 1180.
- (32) (a) Tarantul, A.; Tsukerblat, B.; Müller, A. *Chem. Phys. Lett.* **2006**, *428*, 361. (b) Tarantul, A.; Tsukerblat, B.; Müller, A. *Inorg. Chem.* **2007**, *46*, 161. (c) Tsukerblat, B.; Tarantul, A.; Müller, A. *Phys. Lett.* **2006**, *353*, 48. (d) Tarantul, A.; Tsukerblat, B.; Müller, A. *J. Chem. Phys.* **2006**, *125*, 054714.
- (33) Kanamori, J. In *Magnetism*; Rado, G. T., Suhl, H., Eds.; Academic Press: New York, 1963; Vol. 1, p 127.
- (34) Owen, J.; Harris, E. A. In *Electron Paramagnetic Resonance*; Geshwind, S., Ed.; Plenum Press: New York, 1972.
- (35) Part 2 of this series: Belinsky, M. I. *Inorg. Chem.* **2008**, *47*, 3532.

nonzero components G_x , G_y , G_z of the DM coupling parameters. The solutions of the $[2(S = 1/2) - S = 3/2]$ DM mixing for the trigonal cluster, without an initial ZFS ($D_0 = 0$), were obtained in refs 31 and 32. We will consider the isosceles system with two nonzero components $G_{ij,x'}$ and $G_{ij,z}$ ($G_{ij,y'} = 0$) of the DM coefficients.

The DM exchange mixing of the $S = 1/2$ and $S = 3/2$ states of the isosceles trimer is described by eq 3

$$\begin{aligned} \langle \phi_0(\pm 1/2) \| \Phi(\pm 3/2) \rangle &= \pm 3i(G_{\pm} - \Delta G_{\pm}/3)/4 \\ \langle \phi_1(\pm 1/2) \| \Phi(\pm 3/2) \rangle &= 3(G_{\pm} - \Delta G_{\pm})/4 \\ \langle \phi_0(\pm 1/2) \| \Phi(\mp 1/2) \rangle &= \mp i\sqrt{3}(G_{\pm} - \Delta G_{\pm}/3)/4 \\ \langle \phi_1(\pm 1/2) \| \Phi(\mp 1/2) \rangle &= \sqrt{3}(G_{\pm} - \Delta G_{\pm})/4 \\ \langle \phi_0(\pm 1/2) \| \Phi(3/2, \pm 1/2) \rangle &= i\Delta G_z \sqrt{6} \end{aligned} \quad (5)$$

where $G_{\pm} = (G_x \pm iG_y)/\sqrt{2}$, $G_{12,k'} = G_k$, $\Delta G_{\pm} = (\Delta G_x \pm i\Delta G_y)/\sqrt{2}$, $\Delta G_k = (G_{12,k'} - G_{23,k'})$; $G_{23} = G_{31} \neq G_{12}$ for the isosceles cluster; $\Delta G_{x,y,z} = 0$ in the trigonal cluster. Equation 5 differs from the consideration^{31a,32} by the account of the ΔG distortions. The $[8 \times 8]$ energy matrix of the Hamiltonian (3) in the basis set $\varphi_0(\pm 1/2)$, $\varphi_1(\pm 1/2)$, $\Phi(3/2, M)$ is represented in Table A1 of Appendix A. In the trigonal case, the energies E_i^{\pm} and eigenfunctions Φ_i^{\pm} for the Hamiltonian (3) in magnetic field $H = H_z$ are described by eqs S8 and S9, respectively, of the Supporting Information. In the trigonal cluster, the excited $\Phi(3/2, -3/2)$, $\Phi(3/2, 3/2)$ states are mixed by the DM(x) exchange with the trigonal $\Psi_{1+}^0(-1/2)$, $\Psi_{1-}^0(-1/2)$ states (eq S9), respectively, which diagonalize H_{DM}^0 {GS $E_1^0 = G_z\sqrt{3}/2$ for $G_z < 0$ }. The excited $\Phi(3/2, -1/2)$, $[\Phi(3/2, 1/2)]$ state is mixed by the DM(x) exchange with the $\Psi_{2+}^0(1/2)$ [$\Psi_{2-}^0(-1/2)$] state (eq S9), which diagonalize the DM(z) exchange operator {GS $E_2^0 = -G_z\sqrt{3}/2$ for $G_z > 0$ }. The $\Psi_{1+}^0(-1/2)$, $\Psi_{1-}^0(-1/2)$ { $\Psi_{2+}^0(1/2)$, $\Psi_{2-}^0(-1/2)$ } functions transform according to irreducible representations $\bar{E}\{\bar{A}_1, \bar{A}_2\}$ of the double group D_3 .⁶

Figure 1 plots ZFS and the field dependence of the states of the Hamiltonian (3) for the trigonal Cu_3 cluster with the parameters (in cm^{-1}) of the Heisenberg exchange $J = J_{av} = 2.92$ and DM exchange $G_x = G_z = 0.37$ (Figure 1a), $G_x = G_z = -0.37$ (Figure 1b), $D_0 = 0.010$; $g = 2.02$, $H = H_z$ (H in Tesla). At low magnetic fields H_z , the Zeeman splitting of the $S = 1/2$ states does not depend on the sign of G_z (Figure 1a and b). In the case of $G_z < 0$, Figure 1a, the GS E_1^- mainly represents the $\Psi_{1+}^0(-1/2)$ state ($|-1/2\rangle_+$ in Figure 1a) at low magnetic field, which transforms smoothly in the $\Phi(3/2, -3/2)$ state at high magnetic field (see eq S9 of the Supporting Information). In the case of $G_z > 0$, Figure 1b, the GS E_3^- ($\Psi_{2-}^0(-1/2)$ state, $|-1/2\rangle_-$ in Figure 1b) is crossed by the E_1^- Zeeman level ($\Phi(3/2, -3/2)$) at $H = 5$ T.^{31a} The DM(x) exchange coupling results in the repulsion of the E_1^- and E_1^+ levels (Figure 1) at large magnetic fields H_z or causes the avoided level crossing structure (the tunneling gap^{23a,27,28-32}). The repulsion of the $|3/2, |M| = 3/2\rangle$ Kramers doublet from GS $\Psi_{1+}^0(-1/2)$, $\Psi_{1-}^0(-1/2)$ ($G_z < 0$) $\sqrt{3}$ times differs from the repulsion of the $|3/2, |M| = 1/2\rangle$ doublet

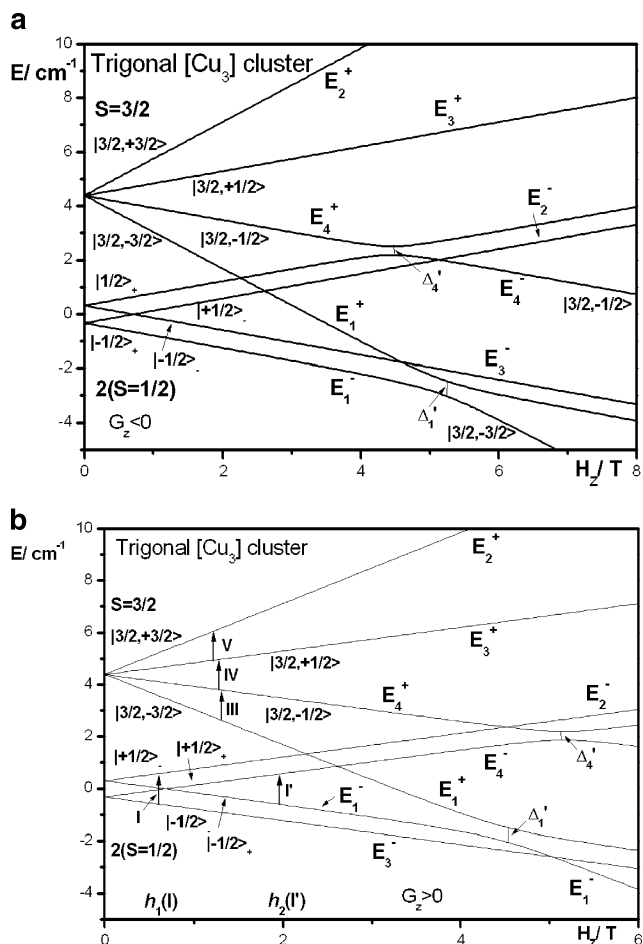


Figure 1. Zero-field and Zeeman splittings of the trigonal states of the $\{\text{Cu}_3\}$ cluster with the small Heisenberg and DM exchange parameters. $J_0 = 2.92 \text{ cm}^{-1}$. (a) $G_{z,x} = -0.37 \text{ cm}^{-1}$. (b) $G_{z,x} = +0.37 \text{ cm}^{-1}$.

from the $\Psi_{2+}^0(1/2)$, $\Psi_{2-}^0(-1/2)$ states, eq 5. This leads to the tunneling gap^{31a,32c} between the lowest E_1^- and E_1^+ levels $\Delta_{12}^{\text{min}} = \Delta_1' = 3|G_x|/2$ in high magnetic field (Figure 1a, $G_z < 0$) and the tunneling gap $\Delta_{56}^{\text{min}} = \Delta_4' = \sqrt{3}|G_x|/2$ between the excited E_4^- and E_4^+ levels. In the case when $G_z > 0$, the tunneling gap $\Delta_{23}^{\text{min}} = \Delta_1'$ exists between the excited E_1^- and E_1^+ levels, Figure 1b.

The importance of the chirality of GS for the explanation of the magnetization at high magnetic fields was discussed in refs 23a and 27. In the case of GS $\Psi_{1+}^0(-1/2)$ ($G_z < 0$), the smooth transformation $\Psi_{1+}^0(-1/2) \rightarrow \Phi(3/2, -3/2)$ at large magnetic fields due to the DM(x) mixing (Figure 1a, eq S9) and the single peak of the differential magnetization were observed for the equilateral V_3 triangle.^{27a} In the case of $\Psi_{2-}^0(-1/2)$ GS ($G_z > 0$), Figure 1b, the crossing $S_{\text{gr}} = 1/2 - S_{\text{gr}} = 3/2$ (E_3^- and E_1^-) takes place without the tunneling gap and the sharp transition $-1/2 \rightarrow -3/2$ takes place in GS at large magnetic fields.^{27a} GS of the $\{\text{Cu}_3\}$ nanomagnet ($G > 0$) was dominantly characterized by a left chirality,^{23a} and the half-step magnetization arises from a different mixing of the spin chirality states to the $S = 3/2$ states.

In Figure 1b, the allowed Q -band EPR transitions for the trigonal cluster are shown schematically by the vertical arrows at low magnetic field H_z . The relative intensities of

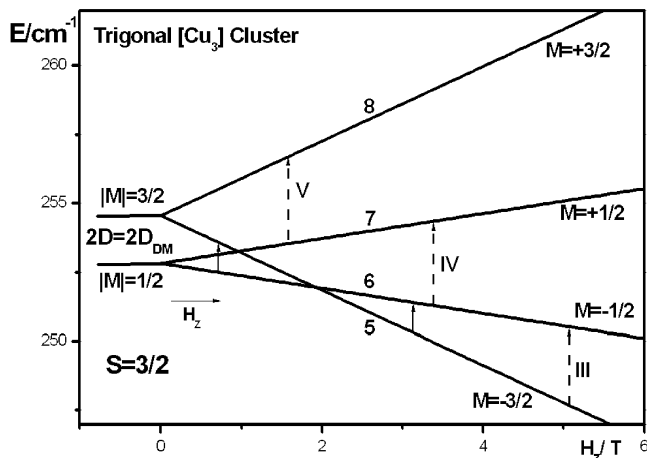


Figure 2. ZFS of the excited $S = 3/2$ state induced by the $DM(x)$ exchange mixing (G_x) in the trigonal Cu_3 cluster with strong Heisenberg and DM exchange coupling. $J_{av} = 168 \text{ cm}^{-1}$, $|G_{z,x}| = 31 \text{ cm}^{-1}$, $D_0 = 0$, $H = H_z$.

the allowed EPR transitions for $S = 3/2$ follow the standard relations $W_{III} = W_V = 0.75$, $W_{IV} = 1$, $W_{ij} = 1/2|\langle \Phi_j | (S_x + iS_y) | \Phi_i \rangle|^2$. In the $2(S = 1/2)$ states of the trigonal cluster, there are only two allowed EPR transitions $E_1^- \rightarrow E_4^-$ ($-1/2)_+ \rightarrow |1/2\rangle_+$) and $E_3^- \rightarrow E_2^-$ ($-1/2)_- \rightarrow |1/2\rangle_-$) with the same intensities $W_{14}(I) = W_{23}(I') = 0.25$ and the resonance fields $h_1(I) = h\nu - \Delta_0$, $h_2(I') = h\nu + \Delta_0$, $h_2 - h_1 = 2\Delta_0$. In the trigonal system, the EPR transitions II ($1 \rightarrow 2$ (3)) and II' (3 (2) $\rightarrow 4$) are symmetry forbidden⁶ $W_{12(13)}(II) = W_{34(24)}(II') = 0$.

In zero magnetic field ($H = 0$), different repulsions of the $|3/2, |M|=3/2\rangle$ and $|3/2, |M|=1/2\rangle$ Kramers doublets from the ground trigonal $\Psi_{1+}^0(-1/2)$, $\Psi_{1-}^0(1/2)$ (\bar{E}) and $\Psi_{2+}^0(1/2)$, $\Psi_{2-}^0(-1/2)$ (\bar{A}_1 , \bar{A}_2) states, respectively (eq S8 in the Supporting Information), results in the DM exchange contribution $2D_{DM}$ to the effective ZFS

$$2D_{\text{eff}} = 2D_0 + 2D_{DM}$$

of the $S = 3/2$ level of the trigonal AFM cluster, where $2D_0$ is the ZFS of the anisotropic exchange origin.^{33,34} The DM exchange contribution $2D_{DM}$ to the cluster ZFS has the form:

$$2D_{DM} = (G_x^2/4J_0)[1 + 2G_z/J_0\sqrt{3}] \quad (6)$$

Since the repulsion of the $|3/2, |M|=3/2\rangle$ and $|1/2, 1/2\rangle$ doublets is $\sqrt{3}$ times stronger than that of the $|3/2, |M|=1/2\rangle$ and $|1/2, 1/2\rangle$ doublets, the $DM(x)$ exchange contribution to ZFS of the $S = 3/2$ excited state is positive for AFM cluster: $E_{DM}(3/2, |M|=3/2) > E_{DM}(3/2, |M|=1/2)$, $D_{DM} > 0$. In the case of $G_x, G_y \neq 0$, the multiplier G_x^2 in eq 6 should be replaced by $(G_x^2 + G_y^2)$. Equation 6 describes the dependence of ZFS on the sign of G_z in the third order of the perturbation theory ($G_k \ll J_0$). The ZFS of the excited $S = 3/2$ state of the V_3 cluster of the V_{15} center induced by the $DM(x,y)$ exchange was obtained^{32c} in the form $2D' = (G_x^2 + G_y^2)/4J$.

For the Cu_3 clusters with small Heisenberg parameter (Figure 1, $J_0 = 2.92 \text{ cm}^{-1}$), ZFS of the $S = 3/2$ state induced by the DM exchange mixing is $2D_{DM} = 0.010 \text{ cm}^{-1}$ for $G_{x,z} = -0.37 \text{ cm}^{-1}$ (Figure 1a) and $2D_{DM} = 0.013 \text{ cm}^{-1}$ for $G_{x,z} = 0.37 \text{ cm}^{-1}$ (Figure 1b) parameters.

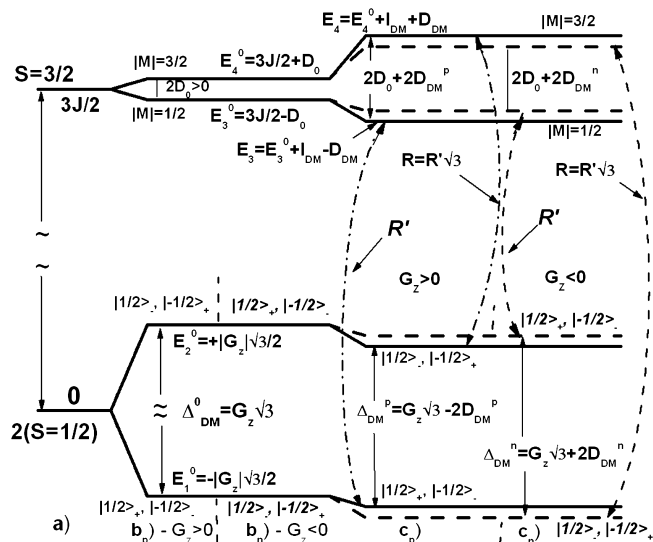


Figure 3. Scheme of the effect of the in-plane (G_x) $DM(x)$ mixing and sign of G_z on ZFS of the excited $S = 3/2$ and ground $2(S = 1/2)$ states of the trigonal AFM cluster. (a) Heisenberg splitting, $G = 0$. (b) Initial zero-field gap $\Delta_{DM}^0 = |G_z|\sqrt{3}$ of GS $2(S = 1/2)$ and ZFS $2D_0$ of the excited $S = 3/2$ state: (b_p) $G_z > 0$, (b_n) $G_z < 0$. (c) Splittings and shifts of the excited and ground states induced by the $DM(x)$ exchange mixing: (c_p) solid lines, $G_z > 0$; (c_n) dashed lines, $G_z < 0$.

For the Cu_3 cluster with strong Heisenberg exchange and DM exchange interaction, the ZFS of the excited $S = 3/2$ state induced by the $DM(x)$ exchange mixing is shown in Figure 2 ($H = H_z$) on an example of the trigonal cluster with $J_0 = 168 \text{ cm}^{-1}$, $|G_{x,z}| = 31 \text{ cm}^{-1}$, $|G_k/J_0| = 0.185$, and $D_0 = 0$. In spite of the large interval $3J_0/2$ between the $2(S = 1/2)$ and $S = 3/2$ states, different $DM(x)$ repulsion of the $|3/2, |M|=3/2\rangle$ and $|3/2, |M|=1/2\rangle$ Kramers doublets from the ground $2(S = 1/2)$ states results in the large DM contribution $2D_{DM}$ to the axial ZFS parameter $2D_{\text{eff}}$ of the $S = 3/2$ state which depends on the sign of G_z : $2D_{DM} = 1.73$ { 1.13 } cm^{-1} for $G_{x,z} = 31$ { -31 } cm^{-1} (Figure 2).

Figure 3 plots schematically the influence of the $DM(x)$ exchange mixing and the sign of G_z on ZFS of the excited $S = 3/2$ state and GS $2(S = 1/2)$. Figure 3a represents the trigonal Heisenberg S states separated by the $3J/2$ interval, $J = J_0$. In Figure 3b ($G_z \neq 0$, $G_x = 0$), the splitting $\Delta_{DM}^0 = |G_z|\sqrt{3}$ of the $2(S = 1/2)$ set is determined by the value of the DM $|G_z|$ parameter and does not depend on the sign of G_z (Figure 3b_p, $G_z < 0$ and Figure 3b_n, $G_z > 0$); an initial ZFS $2D_0$ of the $S = 3/2$ state is determined by the anisotropic exchange. In the case of $G_{z,x} \neq 0$ (Figure 3c), positive G_z DM parameter (Figure 3c_p) results in the ground $|1/2\rangle_{\pm}$ doublet, which is separated from the lowest excited $|3/2, |M|=1/2\rangle$ Kramers doublet by the larger energy interval $(3J + \Delta_{DM}^0 - D_0)/2$ (Figure 3b_p). These doublets experience the smaller repulsion (the dash-dotted arrows in Figure 3c), each from the other, induced by the $DM(x)$ exchange (the nondiagonal $DM(x)$ matrix elements $i\sqrt{3}G_x/4$ in the matrix (A1) of Appendix A are designated schematically as R' in Figure 3c_p). The first excited doublet [$\Psi_{1+}^0(-1/2)$, $\Psi_{1-}^0(1/2)$] is separated by the smaller interval $(3J - \Delta_{DM}^0 + D_0)/2$ from the $|3/2, |M|=3/2\rangle$ doublet ($G_z > 0$, Figure 3b_p), these doublets are characterized by the larger $DM(x)$ repulsion between them ($3iG_x/4$, $R = R'\sqrt{3}$ in Figure 3c_p). This leads

to the larger positive ZFS $2D_{DM}^0$ of the $S = 3/2$ state for positive G_z (solid lines for the $|3/2, |M\rangle$ doublets in Figure 3c_p). For $G_z < 0$, the $[\Psi_{1+}^0(-1/2), \Psi_{1-}^0(1/2)]$ ground doublet is separated by the larger interval $(3J + \Delta_{DM}^0 + D_0)/2$ from the excited $|3/2, |M| = 3/2\rangle$ doublet (Figure 3b_n), these doublets experience the larger DM(x) repulsion, each from the other (dashed arrows in Figure 3c_n, $R = R'\sqrt{3} \sim 3G_x$). The first excited $|\pm 1/2\rangle_{\pm} S = 1/2$ state (Figure 3c_n, $G_z < 0$) is separated by the smaller interval $(3J - \Delta_{DM}^0 - D_0)/2$ from the $|3/2, |M| = 1/2\rangle$ doublet, these doublets experience the smaller repulsion ($R' \sim \sqrt{3}G_x$, dashed arrows in Figure 3c_n). This repulsion leads to the smaller positive ZFS $2D_{DM}^0$ of the $S = 3/2$ state for negative G_z (dashed lines for the $|3/2, |M\rangle$ doublets in Figure 3c_n). Since the chirality of GS $S = 1/2$ is determined by the sign of G_z (Figure 3b), the dependence of the $S = 3/2$ ZFS on the sign of G_z in Figure 3c shows the correlation between the chirality of GS and ZFS $2D_{DM}^0$ of the excited-state induced by the DM exchange mixing.

Due to the repulsion of the $S = 3/2$ and $S = 1/2$ levels at $H = 0$ (Figure 3), the DM(x) exchange also results in the common shifts $\pm l_{DM}$ of these states, respectively, and the splitting $\pm D_{DM}$ of the $2(S = 1/2)$ states additional to the standard $\pm G_z\sqrt{3/2}$ DM(z) exchange splitting (Figure 3c). The zero-field energies of the $S = 3/2$ and $S = 1/2$ states are

$$\begin{aligned} E_1^+ &= E_2^+ \approx 3J/2 + l_{DM} + (D_0 + D_{DM}) \\ E_3^+ &= E_4^+ \approx 3J/2 + l_{DM} - (D_0 + D_{DM}) \\ E_1^- &= E_2^- \approx G_z\sqrt{3/2} - l_{DM} + D_{DM} \\ E_3^- &= E_4^- \approx -G_z\sqrt{3/2} - l_{DM} + D_{DM} \end{aligned} \quad (7)$$

where the common shift $l_{DM} = (G_x^2/8J)[2 + G_zJ/3]$ depends on the G_x and G_z parameters. Different additional shifts of the levels due to the DM(x,y) exchange mixing was described in ref 32c in the form $-(G_x^2 + G_y^2)/8J$ and $-3(G_x^2 + G_y^2)/8J$.

In the case of $G_z < 0$, the $[\Psi_{1+}^0(-1/2), \Psi_{1-}^0(1/2)]$ state is GS with the energy $E_{1,2}^-$ (Figure 3c_n, Figure 1a) and the first $S = 1/2$ excited state $(|\pm 1/2\rangle_{\pm})$ has the energy $E_{3,4}^-$. In the case of $G_z > 0$, the structure of the levels is opposite: the $[\Psi_{1+}^0(+1/2), \Psi_{1-}^0(-1/2)]$ doublet is GS with the energy $E_{3,4}^-$ and $[\Psi_{1+}^0(-1/2), \Psi_{1-}^0(1/2)]$ is the first excited-state with the energy $E_{1,2}^-$ for $G_{z,x} < 0$ (Figure 3c_p, Figure 1b). The resulting splitting of GS $2(S = 1/2)$ is different for $G_z < 0$ [$\Delta(E_{3,4}^- - E_{1,2}^-) = |G_z|\sqrt{3} + 2D_{DM}$] and $G_z > 0$ [$\Delta(E_{1,2}^- - E_{3,4}^-) = G_z\sqrt{3} - 2D_{DM}$] and depends on the sign of G_z and the chirality of GS (Figure 3).

For the trigonal cluster with $J_0 = 168 \text{ cm}^{-1}$, $|G_{x,z}| = 31 \text{ cm}^{-1}$, the DM splitting of the $2(S = 1/2)$ states is (in cm^{-1}) $\Delta = 52$ (54.9) for $G_{x,z} = +31$ (-31) in comparison with an initial splitting $\Delta_{DM}^0 = G_z\sqrt{3} = 53.7 \text{ cm}^{-1}$ induced only by the out-of-plane H_{DM}^Z DM exchange ($|G_z| = 31 \text{ cm}^{-1}$, $G_x = 0$). An additional DM(x) splitting of the $2(S = 1/2)$ states is small: -1.7 cm^{-1} (-3%) and $+1.2 \text{ cm}^{-1}$ ($+2\%$) for $G_z = 31 \text{ cm}^{-1}$ and $G_z = -31 \text{ cm}^{-1}$, respectively, $|G_x| = 31 \text{ cm}^{-1}$. In the case of $G_{x,z} = 31 \text{ cm}^{-1}$, the common shift of the levels induced by the DM(x) exchange mixing is small $l_{DM} = 1.51 \text{ cm}^{-1}$, $l_{DM} \ll 3J_0/2$.

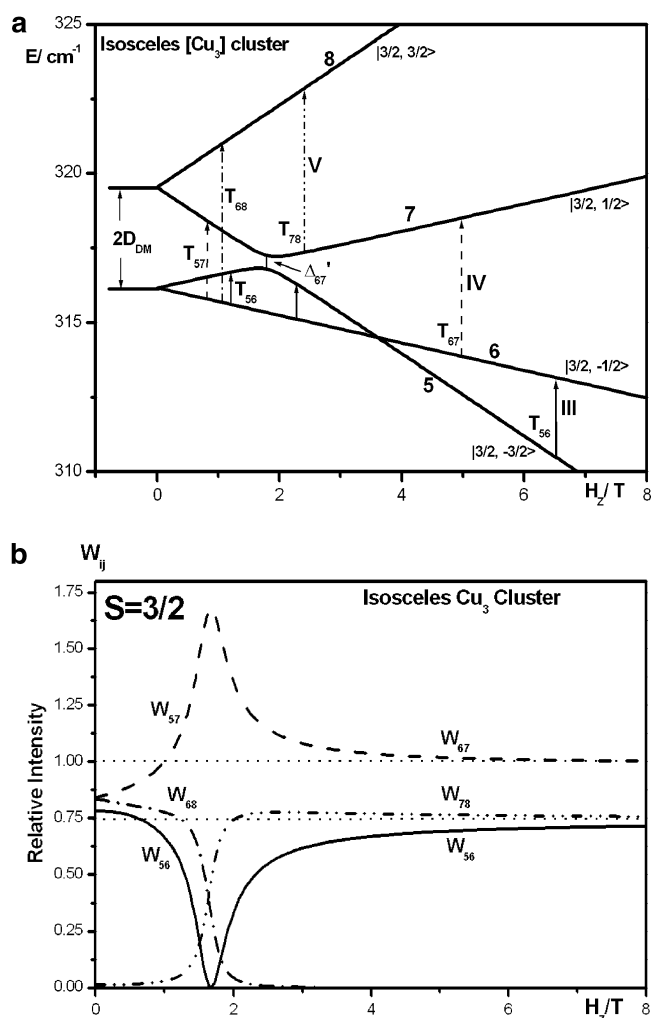


Figure 4. Isosceles Cu_3 cluster; $J_{12} = 252 \text{ cm}^{-1}$, $J_{1,3,2,3} = 189 \text{ cm}^{-1}$, $G_z = G_x = 47 \text{ cm}^{-1}$. (a) ZFS and Zeeman splitting of the $S = 3/2$ state. (b) Field dependence of the relative intensities $W_{ij}(H_z)$ of the allowed EPR transitions for the $S = 3/2$ state.

One can conclude that the description of ZFS of GS $2(S = 1/2)$ of the Cu_3 clusters with strong DM coupling in the framework of the H_{DM}^Z DM(z) model^{6,7,9,18–20} is correct in the case $G_z \neq 0$, $G_{x,y} = 0$ and also even in the case of the presence of the large in-plane DM(x,y) mixing of the $2(S = 1/2)$ and $S = 3/2$ states (with an accuracy 1–3%).

At the same time, ZFS of the $S = 3/2$ state induced by the DM(x) exchange mixing is large (Figure 2). ZFS induced by the DM exchange depends significantly on the orientations of the pair G_{ij} vectors. In the case of $G_z \neq 0$, $G_{x,y} = 0$,^{20a} the effect of the DM mixing on ZFS of the $S = 3/2$ state is absent. In the case of $G_z = 0$, $G_{x,y} \neq 0$, the splitting $2D_{DM}^0$ of the $S = 3/2$ and $2(S = 1/2)$ states has the DM(x) exchange origin.

For the trigonal Cu_3 clusters, the DM(x) exchange mixing of the $S = 1/2$ and $S = 3/2$ states remains the system trigonal: the ZFS Hamiltonian for the $S = 3/2$ has the trigonal form H_{ZFS}^0 (2) with the axial ZFS parameter $D_{\text{eff}} = D_0 + D_{DM}$, the magnetic field dependence for $H = H_z$ is linear (Figure 2) and the intensities of the EPR transitions follow the standard relations ($W_{IV} \cdot W_{III(V)} = 4:3$) characteristic for the $S = 3/2$ state.

3. Isosceles Cu_3 Clusters with the $S = 1/2 - S = 3/2$ Mixing by the DM Exchange

3.1. AFM Cu_3 Clusters with Large Heisenberg Parameters. The AFM Cu_3 clusters, which possess large DM exchange parameters, are characterized by the large δ distortions^{18,19} (Table 1). The δ distortions contribute to an initial ZFS $\Delta_0 = \sqrt{(\delta^2 + 3G_z^2)}$ of the $2(S = 1/2)$ states and coefficients of the wave functions $\Psi_{\pm}(M = \pm 1/2)$ of the isosceles (distorted) Cu_3 cluster with $G_z \neq 0$, $G_{x,y} = 0$ (eqs S5 and S6 of the Supporting Information). In the isosceles Cu_3 cluster with the DM(x) exchange mixing, both $\Psi_{\pm}(M)$ states are mixed with both $|3/2, \pm 3/2\rangle$ and $|3/2, \pm 1/2\rangle$ Kramers sublevels. Thus, for the $M = -1/2$ ground states, the DM mixing has the form

$$\langle \Psi_{\pm}(-1/2) | H_{\text{DM}} | \Phi(3/2, -3/2) \rangle = - (3iG_x/4) \sqrt{\frac{1}{2}(1 \pm G_z \sqrt{3}/\Delta_0)}$$

$$\langle \Psi_{\pm}(-1/2) | H_{\text{DM}} | \Phi(3/2, 1/2) \rangle = \mp (iG_x/4) \sqrt{\frac{3}{2}(1 \mp G_z \sqrt{3}/\Delta_0)} \quad (8)$$

The spin mixing of the $S = 1/2$ and $S = 3/2$ sublevels (eq 8) changes significantly ZFS of the $S = 3/2$ state. The ZFS and Zeeman ($H = H_z$) splitting of the $S = 3/2$ state of the isosceles Cu_3 cluster with the large AFM Heisenberg parameters (in cm^{-1} , $J' = 252$, $J = 189$, $\delta = 63$, $\delta/J_{\text{av}} = 0.3$) and DM exchange parameter¹⁹ ($G_z = 47 \text{ cm}^{-1}$) are shown in Figure 4a for the system with $G_z = G_x$ and $G_{12} = G_{13} = G_{23}$. The DM(x) mixing contribution $2D_{\text{DM}}$ (in cm^{-1}) to ZFS of the $S = 3/2$ state is large $2D_{\text{DM}} = 3.36$ for the isosceles cluster with $G_{z,x} = +47$ in Figure 4a ($2D_{\text{DM}} = 2.03$ for $G_{z,x} = -47$). The estimate using eq 6 with $J_{\text{av}} = 210 \text{ cm}^{-1}$ results in $2D_{\text{DM}} = 3.31\{1.95\} \text{ cm}^{-1}$ for $G_{z,x} = 47 \{-47\} \text{ cm}^{-1}$. In distinction from the trigonal cluster (Figure 2) with the linear field dependence, the DM(x) exchange mixing in the isosceles Cu_3 cluster results in the new peculiarity of the DM mixing: the nonlinear field dependence for $H = H_z$ of the Zeeman sublevels 6 and 7 (formally, $|3/2, M = -3/2\rangle$ and $|3/2, +1/2\rangle$) and the tunneling gap $\Delta_{67}^{\text{min}} = \Delta_{67}' (= 0.455 \text{ cm}^{-1})$ between these levels with $\Delta M = 2$ in the field of their crossing point ($H_z = D/g\mu_B$) for the trigonal cluster (Figure 4a). This nonlinear magnetic behavior for $H = H_z$ is determined by the different admixture of the $S = 1/2$ states to the $|3/2, +1/2\rangle$ and $|3/2, -3/2\rangle$ states and resulting mixing of the $\Phi(3/2, +1/2)$ and $\Phi(3/2, -3/2)$ states with $\Delta M = 2$.

The mixing of the $S = 3/2$ states with $\Delta M = 2$ is usually described by the rhombic term $E_0(S_x^2 - S_y^2)$ in the ZFS Hamiltonian:²⁶

$$H_{\text{ZFS}} = D_0[S_z^2 - S(S+1)/3] + E_0(S_x^2 - S_y^2) \quad (9a)$$

The ZFS of the $S = 3/2$ level described by the Hamiltonian (9a) and the nonlinear field dependence for $H = H_z$ has the form shown in Figure 4a with the repulsion between the 6 and 7 Zeeman levels and the $\Delta_{67}^{\text{min}} = 2E_0\sqrt{3}$ tunneling gap. Using the interval Δ_{67}' (Figure 4a), one obtains the rhombic

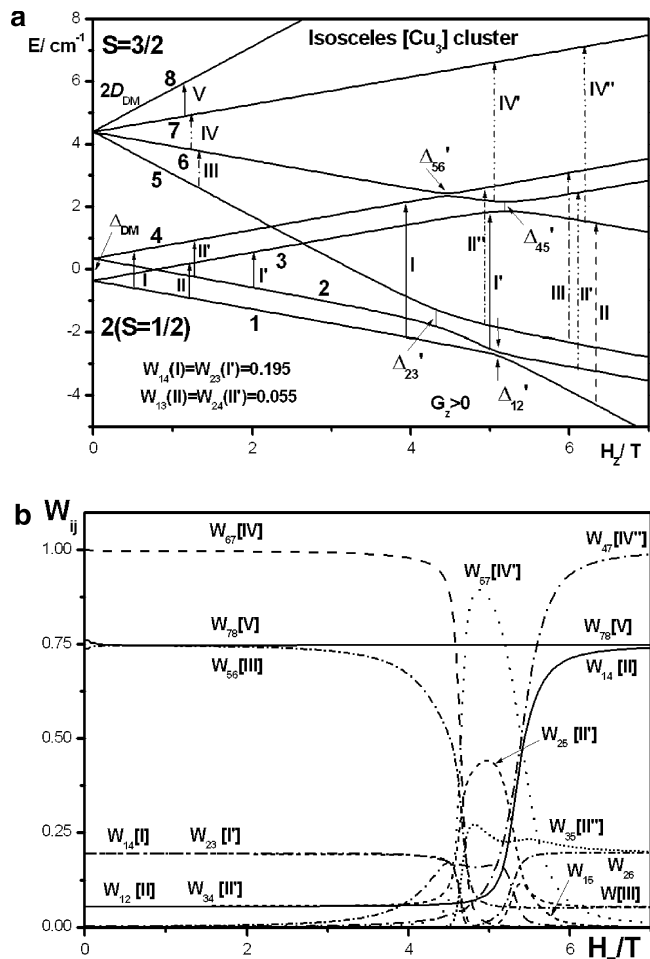


Figure 5. Isosceles Cu_3 cluster; $J_{12} = 3.143 \text{ cm}^{-1}$, $J_{13,23} = 2.808 \text{ cm}^{-1}$, $G_{z,x} = 0.368 \text{ cm}^{-1}$. (a) ZFS, Zeeman splitting ($H = H_z$) and allowed EPR transitions. (b) Field dependence of the relative intensities $W_{ij}(H_z)$ of the allowed EPR transitions.

ZFS parameter $E_{\text{DM}} = 0.131 \text{ cm}^{-1}$ of the DM(x) exchange mixing origin, $E_{\text{DM}} \ll D_{\text{DM}}$. In the isosceles Cu_3 cluster with the DM(x) exchange mixing, the δ distortion leads to the new rhombic-type anisotropy of the $S = 3/2$ state induced by the DM exchange which corresponds to the isosceles geometry.

The nonlinear magnetic behavior (Figure 4a) determines the resonance fields of the EPR transitions and leads to the complicated field dependence $W_{ij}(H_z)$ of the intensities of the allowed EPR transitions for the $S = 3/2$ state, shown in Figure 4b for the cluster with $J' = 252$, $J = 189$, $G_{z,x} = 47 \text{ cm}^{-1}$. The relative intensities $W_{ij}(H_z)$ differ significantly from the standard relation $W_{\text{IV}} = 1$, $W_{\text{III(V)}} = 0.75$ (dotted straight lines in Figure 4b) characteristic for the $S = 3/2$ EPR transitions at $H = H_z$, Figure 2. The intensities follow these standard relations only at high magnetic fields where the DM exchange effect are suppressed by the field.

3.2. AFM Cu_3 Clusters with Small AFM Exchange and DM Exchange Parameters. Figure 5a plots the energy levels for the isosceles Cu_3 cluster (matrix A1 of Appendix A) with the exchange parameters (in cm^{-1}) $J_{12} = 3.143$, $J_{13,23} = 2.808$, $\delta = 0.335$, $J_{\text{av}} = 2.92$, $G_{z,x} = +0.368$, $G_y = 0$, $\Delta_0 = 0.720$, $g = 2.06$, and the crossing of the $S = 3/2$ and $S = 1/2$ levels at large magnetic field (5 T). The ZFS of the $S =$

3/2 state induced by the DM(x) exchange (G_x) mixing is $2D_{DM} = 0.0134 \text{ cm}^{-1}$ in Figure 5a; the ZFS of the 2(S = 1/2) group is $\Delta = 0.708 \text{ cm}^{-1}$ ($< \Delta_0$, in accordance with Figure 3c).

The DM(x) admixture (eq 8) changes the picture of the field dependence in the area of the crossing points in comparison with the trigonal cluster. In the isosceles Cu_3 cluster, the tunneling gaps Δ_{ij}^{min} ($= \Delta_{ij}'$ in Figure 5a) in the levels crossing points at large magnetic fields depend on the values of δ , $G_{x,z}$, and on the sign of G_z , Figure 5a. The values of the tunneling gaps between the levels 1 and 2, 2 and 3, 4 and 5, and 5 and 6 (in cm^{-1}) are $\Delta_{12}' = 0.124$, $\Delta_{23}' = 0.534$, $\Delta_{45}' = 0.31$, $\Delta_{56}' = 0.08$, respectively, in Figure 5a for positive DM parameters $G_{x,z}$. These tunneling gaps are described by eq 9b

$$\begin{aligned} \Delta_{12(23)'} &\approx 1.5|G_x|\{0.5[1 - (+)G_z\sqrt{3}/\Delta]\}^{1/2} \\ \Delta_{45(56)'} &\approx 0.5|G_x|\{0.5[1 - (+)G_z\sqrt{3}/\Delta]\}^{1/2} \end{aligned} \quad (9b)$$

In the case of $G_x \neq 0$, $G_y \neq 0$, the multiplier $|G_x|$ in eq 9b should be replaced by $\sqrt{(G_x^2 + G_y^2)}$. The DM(x) mixing in isosceles cluster (Figure 5a) results in (i) the appearance of the tunneling gaps between the levels, which are crossed in the trigonal system, even in the presence of the DM(x) mixing (E_3^- and E_1^+ , E_1^+ and E_4^- in Figure 1a; E_3^- and E_1^- , E_2^- and E_4^+ in Figure 1b) and (ii) the reduction of the tunneling gaps $\Delta_1' = 3|G_x|/2$, $\Delta_4' = \sqrt{3}|G_x|/2$, characteristic for the trigonal system ($\Delta_{\text{min}}(E_1^- - E_1^+)$ and $\Delta_{\text{min}}(E_4^- - E_4^+)$), respectively, in Figure 1a and b).

For the isosceles cluster with the Heisenberg parameters (in cm^{-1}) $J' = 3.143$, $J = 2.808$, $\delta = 0.335$ and negative DM parameters $G_{x,z} = -0.368$, the calculations (Table A1 of Appendix A) results in ZFS $\Delta_{DM} = 0.729$ for GS 2(S = 1/2) and $2D_{DM} = 0.010$ for excited S = 3/2 state. The relations $\Delta_{DM} > \Delta_0$ and $2D_{DM}(G_z < 0) < 2D_{DM}(G_z > 0)$ take place, in accordance with Figure 3. The tunneling gaps (in cm^{-1}) $\Delta_{12}' = 0.535$, $\Delta_{23}' = 0.124$, $\Delta_{45}' = 0.075$, and $\Delta_{56}' = 0.310$ for $G_{x,z} < 0$ are well described by eq 9b. This consideration shows that the tunneling gaps depend on the chirality of GS: $\Delta_{12}' < \Delta_{23}'$, $\Delta_{45}' > \Delta_{56}'$ for $G_z > 0$ and $\Delta_{12}' > \Delta_{23}'$, $\Delta_{45}' < \Delta_{56}'$ for $G_z < 0$.

The comparison of the repulsion gaps Δ_{12}' and Δ_{23}' , which may be observed experimentally in the area of the crossing points, allows one to determine the sign of the G_z parameter from 9b and, as a result, the spin chirality of the ground state.

4. ZFS and Intensities of the EPR Transitions in the Cu_3 Clusters with the Crossing of the S = 3/2 and S = 1/2 Levels at High Magnetic Fields

For the $\{\text{Cu}_3\}$ nanomagnet^{23a} with the Heisenberg parameters $J_{12} = 3.143 \text{ cm}^{-1}$, $J_{13} = J_{23} = 2.808 \text{ cm}^{-1}$, Choi et al.^{23a} used three DM exchange parameters $G_x = G_y = G_z = 0.368 \text{ cm}^{-1}$ for the explanation of the magnetic and EPR data. The contribution of the DM mixing to ZFS was not considered in ref 23a. The account of the two in-plane components $G_x = G_y = 0.368 \text{ cm}^{-1}$ of the DM exchange in the calculations of the energy matrix (Table A1 in Appendix

A) with $G_z = +0.368 \text{ cm}^{-1}$, results in the energy levels, shown in Figure 5a, with ZFS of the S = 3/2 state $2D_{DM} = 0.0265 \text{ cm}^{-1}$ of the DM(x,y) exchange origin, ZFS $\Delta_{DM} = 0.6961 \text{ cm}^{-1}$ of GS 2(S = 1/2), and the tunneling gaps $\Delta_{12}' = 0.164 \text{ cm}^{-1}$ [$H_z = 5 \text{ T}$], $\Delta_{23}' = 0.751 \text{ cm}^{-1}$ [$H_z = 4.4 \text{ T}$], $\Delta_{12}' < \Delta_{23}'$. The tunneling gaps Δ_{12}' and Δ_{23}' are described by eq 9b with the multiplier $\sqrt{(G_x^2 + G_y^2)}$ instead of $|G_x|$. In the case of $G_z = -0.368 \text{ cm}^{-1}$, the splittings are the following $2D_{DM} = 0.0200 \text{ cm}^{-1}$, $\Delta_{DM} = 0.7368 \text{ cm}^{-1}$, $\Delta_{12} = 0.750 \text{ cm}^{-1}$ ($H_z = 5.12 \text{ T}$), $\Delta_{23} = 0.166 \text{ cm}^{-1}$ ($H_z = 4.64 \text{ T}$), $\Delta_{12}' > \Delta_{23}'$. Our result concerning the tunneling gaps Δ_{ij}' is not consistent with the result in Figure 4 ($H||Z$) of ref 23a where correlations between the tunneling gaps are $\Delta_{12}' > \Delta_{23}'$, $\Delta_{45}' < \Delta_{56}'$ for $G_z > 0$ for the $\{\text{Cu}_3\}$ nanomagnet. These correlations between the tunneling gaps ($\Delta_{12}' > \Delta_{23}'$, $\Delta_{45}' < \Delta_{56}'$) correspond to the negative G_z parameter.

The value of the $2D_{DM}$ contribution to the isosceles cluster ZFS parameter $2D_{\text{eff}}$ can be estimated using eq 6 with the average parameter $J_{\text{av}} = 2.92 \text{ cm}^{-1}$ and the multiplier $(G_x^2 + G_y^2)$ instead of G_x^2 : $2D_{DM} = 0.0263 \text{ cm}^{-1}$ for $G_{x,y,z} = +0.368 \text{ cm}^{-1}$.

The zero-field gap $2D_e = 0.0662 \text{ K} = 0.0460 \text{ cm}^{-1}$ for the S = 3/2 state of the $\{\text{Cu}_3\}$ nanomagnet observed in EPR²³ was explained by the anisotropic exchange contribution.^{23a} The value $2D_e$ of ZFS was used^{23a} to estimate the exchange anisotropy $A = |J_x - J_z| = 0.6 \text{ K}$. Our calculation of the contribution $2D_{DM}$ to ZFS induced by the in-plane DM(x,y) exchange mixing shows that ZFS $2D_{DM} = 0.0265 \text{ cm}^{-1}$ ($G_{x,y,z} = +0.368 \text{ cm}^{-1}$) contributes 58% of the value of the experimentally observed ZFS $2D_e$. The axial ZFS $2D_0$ of the anisotropic exchange origin contributes 42% to total ZFS $2D_e$ ($2D_{AN} = 2D_0 = 2D_e - 2D_{DM}$) that allows the estimation of the exchange anisotropy ($J_z - J_x$) = $2D_0 = 0.0195 \text{ cm}^{-1} = 0.028 \text{ K}$ which is significantly smaller than the estimate in ref 23a. Large DM(x,y) exchange contribution $2D_{DM}$ to the effective cluster ZFS $2D_{\text{eff}}$ should be taken into account in the conclusion, relating to the origin of the S = 3/2 ZFS and the exchange anisotropy.

ZFS $\Delta_{DM} = 0.696 \text{ cm}^{-1}$ of GS 2(S = 1/2) in the DM model with the DM(x,y) mixing ($G_{x,y,z} = 0.368$, $\delta = 0.335$ (cm^{-1})) is close (97%) to ZFS $\Delta_0 = \sqrt{(\delta^2 + 3G_z^2)} = 0.720 \text{ cm}^{-1}$ induced only by the DM(z) coupling ($G_z = 0.368 \text{ cm}^{-1}$, $G_{x,y} = 0$). The zero-field GS wave function $\Psi_{-}(1/2, -1/2)_{H=0} = 0.858\varphi_0(-1/2) - i0.511\varphi_1(-1/2) - i0.020\Phi(3/2, -3/2) + i0.046\Phi(3/2, 1/2)$ of the isosceles cluster demonstrates the admixture of both $|3/2, -3/2\rangle$ and $|3/2, +1/2\rangle$ excited states. The coefficients of the φ_0 , φ_1 functions (S = 1/2, $M = -1/2$) in the GS wave function $\Psi_{-}(1/2, -1/2)_{H=0}$ are very close to the coefficients $a_+ = \sqrt{[1/2(1 + \delta/\Delta_0)]}$ ($= 0.856$) and $a_- = \sqrt{[1/2(1 - \delta/\Delta_0)]}$ ($= 0.517$), which describe the GS function $\Psi_{-}(-1/2) = a_+\varphi_0(-1/2) - ia_-\varphi_1(-1/2)$ of the isosceles trimer (see eqs S5 and S6 in the Supporting Information) with G_z (0.368 cm^{-1}) and δ (0.335 cm^{-1}) parameters without the DM(x,y) admixture ($G_{x,y} = 0$). It shows that even large DM(x,y) admixture in the isosceles clusters has a small influence on the GS magnetic behavior at low magnetic fields.

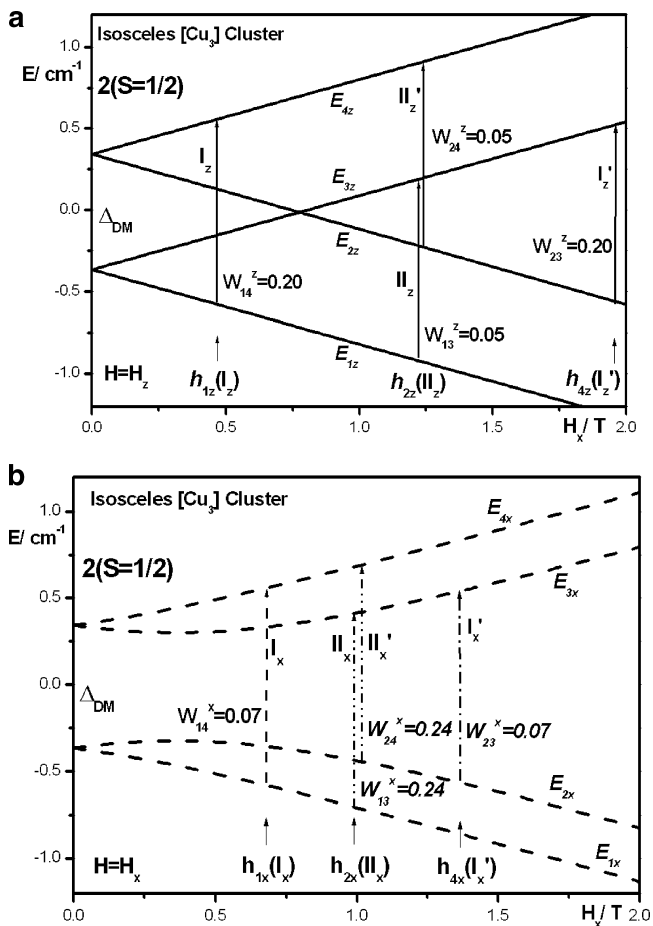


Figure 6. Splitting of the $2(S = 1/2)$ states of the isosceles Cu_3 cluster and the allowed Q-band EPR transitions. $J_{12} = 3.143 \text{ cm}^{-1}$, $J_{13,23} = 2.808 \text{ cm}^{-1}$, $G_{z,x} = 0.368 \text{ cm}^{-1}$. (a) $H = H_z$, solid lines. (b) $H = H_x$, dashed lines.

In Figure 5a, the allowed EPR transitions are shown by the vertical arrows. The field dependence of the relative intensities of the allowed EPR transitions ($H = H_z$) for the cluster with the exchange parameters (in cm^{-1}) $J' = 3.143$, $J = 2.808$, $\delta = 0.335$, $G_{x,z} = 0.368$, $G_y = 0$ (Figure 5a) are shown in Figure 5b. The relative intensities $W_{ij}(H_z)$ of the EPR transitions are changed significantly in the area of the mixing of the spin levels at high magnetic fields (Figure 5b) where the EPR transitions between the mixed spin states take place. At low magnetic fields, $H < 3 \text{ T}$ (X-band and Q-band EPR), the intensities of the EPR transitions for the $S = 3/2$ and $2(S = 1/2)$ groups do not depend on the DM(x) exchange mixing and the value of magnetic field H_z (Figure 5b). At low fields $H = H_z$, there are four allowed EPR transitions I ($1 \rightarrow 4$), I' ($2 \rightarrow 3$), II ($1 \rightarrow 3$), II' ($2 \rightarrow 4$) in the $2(S = 1/2)$ group (Figure 6a). The intensities of the EPR transitions $W_{14}(\text{I}) = W_{23}(\text{I}') = 0.195$, $W_{13}(\text{II}) = W_{24}(\text{II}') = 0.055$ calculated, using Table A1 of Appendix A for $H = H_z$, are very close to the relations $W_{14}^Z(\text{I}) = 0.197$, $W_{13}^Z(\text{II}) = 0.053$, which are obtained, using the equation

$$W_{14}^Z(\text{I}) = W_{14}^Z(\text{I}') = 3G_z^2/4\Delta_0^2, \\ W_{13}^Z(\text{II}) = W_{24}^Z(\text{II}') = \delta^2/4\Delta_0^2 \quad (10)$$

for the considered exchange parameters. Equation 10 was obtained for the system without the DM(x) mixing of the $2(S = 1/2)$ and $S = 3/2$ states ($G_{x,y} = 0$).^{6,7} Figure 5b shows

that the intensities of the X-band and Q-band EPR transitions (at low magnetic fields $H = H_z$) are well described by the DM(z) exchange model without taking into account the in-plane DM(x) mixing, both in the cases of the large DM exchange^{18–20} and small DM exchange^{23a} parameters.

For the isosceles cluster, the field dependence ($H = H_x$ in the plane of the cluster) of the relative intensities of the allowed EPR transitions for the X- and Q-band EPR may also be described by the DM(z) exchange model without taking into account the DM(x) mixing. In this case, the field dependence of the relative intensities of the allowed EPR transitions⁶ for $H = H_x$ ($h_x = g\mu_B H_x$) has the form

$$W_{14}^X(\text{I}_X) = 0.75G_z^2/[(\delta + h_x)^2 + 3G_z^2],$$

$$W_{23}^X(\text{I}_X') = 0.75G_z^2/[(\delta - h_x)^2 + 3G_z^2],$$

$$W_{13}^X(\text{II}_X) = W_{24}^X(\text{II}_X') = 0.125\{1 + (3G_z^2 - \delta^2 + h_x^2)/[(\Delta_0^2 + h_x^2)^2 - 4\delta^2 h_x^2]^{1/2}\},$$

$$W_{12}^X = W_{34}^X = 0.125\{1 - (3G_z^2 - \delta^2 + h_x^2)/[(\Delta_0^2 + h_x^2)^2 - 4\delta^2 h_x^2]^{1/2}\} \quad (11)$$

An increase of H_x results in (i) the strong decrease of the intensities $W_{14}^X(\text{I}_X)$, $W_{23}^X(\text{I}_X')$, $W_{12}^X = W_{34}^X$ of the $S = 1/2$ EPR transitions $T_{14}(\text{I}_X)$, $T_{23}(\text{I}_X')$, $T_{12}^X = T_{34}^X$ and (ii) an increase of the intensities $W_{13}^X(\text{II}_X)$, $W_{24}^X(\text{II}_X')$ of the EPR transitions $T_{13}(\text{II}_X)$ and $T_{24}(\text{II}_X')$ up to its maximal values ~ 0.25 characteristic for the isotropic system. The relation between the intensities of the EPR transitions $T_{14}(\text{I}_X)$ and $T_{13}(\text{II}_X)$ at their resonance fields is $W_{14}^X(\text{I}_X):W_{13}^X(\text{II}_X) = 0.07:0.24$ for $H = H_x$ (Figure 6b).

In Figure 6 for the $\{\text{Cu}_3\}$ cluster with the exchange parameters of Figure 5, the Zeeman splittings for $H = H_z$ (Figure 6a, solid lines) and $H = H_x$ (dashed curves in Figure 6b) as well as the allowed Q-band EPR transitions are compared each with others. The allowed EPR transitions I and II for $H = H_z$ ($H = H_x$) are marked as I_z , II_z (I_x , II_x) in Figure 6a {Figure 6b}. For the Q-band EPR ($h\nu = 1.13 \text{ cm}^{-1}$), the resonance fields of the EPR transitions for $H = H_z$ are determined by the relations $h_{1z}(\text{I}) = h\nu - \Delta_0$, $h_{2z}(\text{II}) = h\nu$, $h_{3z}(\text{II}') = h\nu$, $h_{4z}(\text{I}') = h\nu + \Delta_0$ (Figure 6a). Due to the linear field dependence of the $S = 1/2$ levels for $H = H_z$ (Figure 6a) and the nonlinear field behavior for $H = H_x$ (Figure 6b), the EPR line I_z of the EPR transition $1 \rightarrow 4$ $\{T_{14}(\text{I}_z)\}$, which is observed at the resonance field $h_{1z}(\text{I}_z)$ for $H = H_z$ (Figure 6a), is shifted in the area of the higher fields in Figure 6b, $h_{1z}(\text{I}_z) < h_{1x}(\text{I}_x)$ (the resonance field is $h_{1x}(\text{I}_x) = \{[(h\nu)^2 - 3G_z^2]^{1/2} - \delta\}$ for $H = H_x$). The EPR line of the transition II ($1 \rightarrow 3$) $\{T_{13}(\text{II}_z)\}$, which is observed at the resonance field $h_{2z}(\text{II}_z)$ for $H = H_z$ (Figure 6a), is shifted in the area of the lower fields in Figure 6b, $h_{2x}(\text{II}_x) < h_{2z}(\text{II}_z)$ (the resonance field $h_{2x}(\text{II}_x) = \{[(h\nu)^2 - 3G_z^2]^{1/2} + \delta\}$ for $H = H_x$ (ref 6)). The EPR line of the transition II_z' ($2 \rightarrow 4$) in Figure 6a is also shifted in the area of the lower field (II_x') Figure 6b under the change of the magnetic field $H_z \rightarrow H_x$.

Strong angle variation of the EPR resonance fields of the $2(S = 1/2)$ group of the $\{\text{Cu}_3\}$ nanomagnet was observed

by Choi et al.^{23a} the EPR line I_Z (the transition $1 \rightarrow 4$, H_z) is shifted in the area of the higher fields under the angle variation $H_z \rightarrow H_x$, whereas the EPR lines II_Z , II'_Z are shifted in the area of the lower fields for $H_z \rightarrow H_x$.^{23a} The intensities $W_{14}^Z(I)$, $W_{13}^Z(II)$, and $W_{24}^Z(II')$ of the observed^{23a} EPR transitions $1 \rightarrow 4$, $1 \rightarrow 3$, and $2 \rightarrow 4$ arising from the $2(S = 1/2)$ group of levels of the $\{Cu_3\}$ nanomagnet are comparable to each other and are 1 order of magnitude weaker than that of the $S = 3/2$ state.^{23a} Choi et al.^{23a} suggested that this is due to the reduced magnitude of spin. The influence of the DM exchange and distortions on the intensities of the EPR transitions was not considered in ref 23a.

Our calculations, with the parameters used in ref 23a, result in the following relative intensities of the Q-band EPR transitions: for the $S = 3/2$ group $W_{III} = W_{IV} = 0.74$, $W_{IV} = 1$; for the $2(S = 1/2)$ group $W_{14}^Z(I) = 0.195$, $W_{13}^Z(II) = W_{24}^Z(II') = 0.055$ for $H = H_z$ and $W_{14}^Z(I_X):W_{13}^Z(II_X) = 0.07:0.24$ for $H = H_x$ (Figures 5 and 6). In both orientations H_z and H_x , the intensity $W_{14}(I)$ of the EPR transition $1 \rightarrow 4$ differs more than 3 times from the intensity $W_{13}(II)$ of the transition $1 \rightarrow 3$ for the set of the δ and G parameters used in ref 23a. To obtain the comparable intensities one can use the correlations between the intensities $W(I)$ and $W(II)$ which are governed by δ and G_z (eqs 10 and 11). The condition, that the EPR transitions I, I' and II, II', arising from the $2(S = 1/2)$ group, are comparable to each other, as was observed in EPR experiment,^{23a} results in the relation $\delta \approx |G_z|\sqrt{3}$ between the exchange parameters that differs from the relation $\delta/G_z = 0.91$ in ref 23a. In this case ($\delta = |G_z|\sqrt{3}$), the intensities of the EPR transitions for $H = H_z$ in the $2(S = 1/2)$ group $W_{14}^Z(I) = W_{23}^Z(I') = W_{13}^Z(II) = W_{24}^Z(II') = 0.125$ are 8 times weaker than that of the transition $W_{IV} = 1$.

For the pure Heisenberg isosceles system ($G = 0$), the relative intensities of the EPR transitions are $W_{III} = W_{IV} = 0.75$, $W_{IV} = 1$; $W_{13}^Z(II) = W_{24}^Z(II') = 0.25$ for $H = H_z$ and $H = H_x$, the EPR transitions $1 \rightarrow 4$ and $2 \rightarrow 3$ are symmetry forbidden.

The angle dependence of the EPR transitions in the Cu_3 cluster with large G_z was described^{20a} by the DM(z) exchange model with $J = 210$, $G_z = 36$, $\delta = 17.5$ (cm^{-1}).

Relative intensities of the X- and Q-band EPR transitions, their angle dependence and resonance fields are described by the out-of-plane DM exchange model (G_z), the influence of the G_x , G_y DM mixing is small at low magnetic fields.

5. Different G_{ij} Parameters in the Isosceles Cu_3 Cluster

The other effect of the large δ distortion in the isosceles Cu_3 clusters is connected with the proportionality of the pair DM exchange parameters to the Heisenberg exchange parameters:²⁵ $|G_{ij}| \sim (\Delta g/g)J_{ij}$. Thus, for example, for the Cu_3 cluster with the Heisenberg parameters¹⁹ (in cm^{-1}) $J_{12} = 252$, $J_{13} = J_{23} = 189$, $\delta = 63$, the relation between the pair DM exchange parameters should be $G_{12}/G_{23} = J_{12}/J_{23} = 1.33$, $G_{31} = G_{23}$. Using the $G_z = 47$ cm^{-1} parameter¹⁹ as an average value ($G_z = (G_{12,z} + G_{23,z} + G_{31,z})/3$), one obtains $G_{12,z} = 56.4$ cm^{-1} , $G_{23,z} = G_{31,z} = 42.3$ cm^{-1} and $\Delta G_z = (G_{12,z} - G_{23,z}) = 14.1$ cm^{-1} . In this case, the coefficients of the DM mixing (eq 3) depend on ΔG_k . Thus, the difference

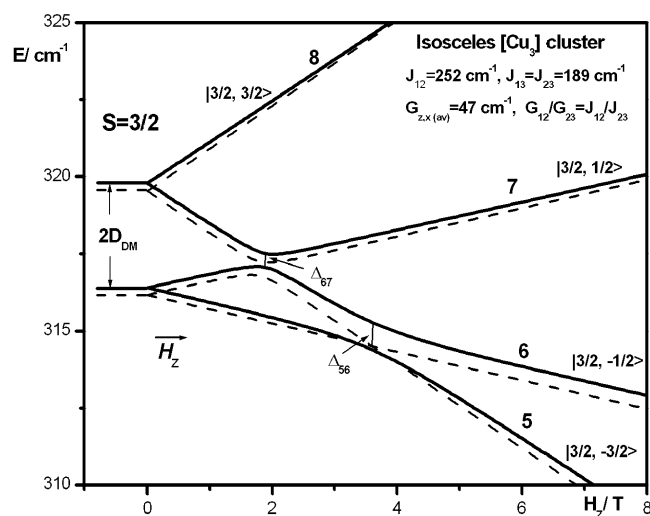


Figure 7. ZFS, tunneling gaps, and field dependence of the $S = 3/2$ levels (solid curves) of the isosceles AFM Cu_3 cluster with the difference ΔG_z of the pair out-of-plane DM parameters (in cm^{-1}) $G_{12,z} = 56.4$, $G_{23,z} = 42.3$, induced by the large δ distortion. $J_{12} = 252$, $J_{13,23} = 189$, $G_{z,(av)} = 47$; $H = H_z$. Dashed curves $\Delta G_z = 0$.

ΔG_z of the pair $G_{ij,z}$ DM parameters results in the mixing of $|S = 1/2, M = \pm 1/2\rangle$ ($S_{12} = 0$) and $|3/2, M = \pm 1/2\rangle$ states with the same total spin projection M (eq 5, the ΔG_z term in the matrix (A1) in Appendix A). The ΔG_z DM(z) exchange mixing of the $S = 1/2$ and $S = 3/2$ states with $\Delta M = 0$ differs from the in-plane (G_x) DM(x) mixing (with $\Delta M = \pm 1$) considered in section 4. The ΔG_z term results in the ΔG_z repulsion of GS $|1/2\rangle$ ($S_{12} = 0$, M) and excited $|3/2, M\rangle$ state and, as a result, in an additional magnetic anisotropy (Figure 7, the solid curves): the nonlinear magnetic behavior of the Zeeman levels 5 and 6 (formally, the $|3/2, -3/2\rangle$ and $|3/2, -1/2\rangle$ states, $|\Delta M| = 1$) and tunneling gap $\Delta_{56}' = \Delta_{56}^{\min} = \Delta_{\min}(E_6 - E_5) = 0.893$ cm^{-1} between these states in the area of their crossing in the case $\Delta G_z = 0$ ($\Delta_{56}^{\min} > \Delta_{67}^{\min} = 0.436$ cm^{-1}). The dashed lines in Figure 7 plot the ZFS, levels and the $|3/2, -3/2\rangle - |3/2, -1/2\rangle$ crossing in the case $\Delta G_z = 0$. This nonlinear magnetic behavior and tunneling gap Δ_{56}' are not described by the standard ZFS Hamiltonian (9a). The ΔG_z repulsion leads also to the shift of the $S = 3/2$ states (Figure 7) and the slight increase of ZFS.

6. DM Exchange Mixing in Ferromagnetic Cu_3 Clusters

The FM Cu_3 clusters ($J_0 = -109$ cm^{-1}) are characterized by the large ZFS of the ground $S = 3/2$ state.^{21a} In the trigonal FM Cu_3 clusters ($J_0 < 0$), the ground $S = 3/2$ state (4A_2 term) is separated by the Heisenberg interval $3J_0/2$ from the excited $2(S = 1/2)$ group (2E term). This large ZFS can be related^{21a} to the strong DM coupling ($|G_z| = 42$ cm^{-1}) and large DM(z) splitting $\Delta_0 = |G_z|\sqrt{3}$ of the excited 2E state. In the case if the DM(x) interaction exists, the calculation of the DM(x) mixing of GS $S = 3/2$ and excited $2(S = 1/2)$ states for the FM cluster results in the DM contribution to ZFS of GS 4A_2 in the form

$$2D_{DM}' = -(G_x^2/4J_0)[1 - 2G_z J_0 \sqrt{3}] \quad (12)$$

In this case, the DM(x) exchange mixing of GS $S = 3/2$ and excited $2(S = 1/2)$ states leads to the negative contribution

Table A1^a

$\varphi_0(-1/2)$	$\varphi_0(1/2)$	$\varphi_1(-1/2)$	$\varphi_1(1/2)$	$\Phi(-3/2)$	$\Phi(-1/2)$	$\Phi(1/2)$	$\Phi(3/2)$
$-1/2(\delta + h_z)$	$1/2h_-$	$-i\sqrt{3}G_z/2$	$i\Delta'G_x$	$-i3G_x'$	$-i\sqrt{2}\Delta'G_z$	$i\sqrt{3}G_x'$	
$1/2h_+$	$-1/2(\delta - h_z)$	$i\Delta'G_x$	$i\sqrt{3}G_z/2$		$-i\sqrt{3}G_x'$	$-i\sqrt{2}\Delta'G_z$	$i3G_x'$
$i\sqrt{3}G_z/2$	$-i\Delta'G_x$	$1/2(\delta - h_z)$	$1/2h_-$	$3G_x''$		$\sqrt{3}G_x''$	
$-i\Delta'G_x$	$-i\sqrt{3}G_z/2$	$1/2h_+$	$1/2(\delta + h_z)$		$\sqrt{3}G_x''$		$3G_x''$
$i3G_x'$		$3G_x''$		$\Delta_1 + D_0 - 3h_z/2$	$\sqrt{3}h_-/2$		
$i\sqrt{2}\Delta'G_z$	$i\sqrt{3}G_x'$		$\sqrt{3}G_x''$	$\sqrt{3}h_+/2$	$\Delta_1 - D_0 - h_z/2$	h_-	
$-i\sqrt{3}G_x'$	$i\sqrt{2}\Delta'G_z$	$\sqrt{3}G_x''$	$3G_x''$		h_+	$\Delta_1 - D_0 + h_z/2$	$\sqrt{3}h_-/2$
	$-i3G_x'$					$\sqrt{3}h_+/2$	$\Delta_1 + D_0 + 3h_z/2$

^a Where $\Delta_1 = (J_{12} + J_{13} + J_{23})/2$, $G_x' = (G_x - \Delta G_x/3)/4\sqrt{2}$, $G_x'' = (G_x - \Delta G_x)/4\sqrt{2}$, $\Delta'G_k = \Delta G_k/2\sqrt{3}$, $\Delta G_k = G_{12,k} - G_{23,k}$, $G_{23} = G_{31}$, $k = x, z$; $h_z = g\mu_B H_z$, $h_{\pm} = g\mu_B(H_x \pm iH_y)$, $\Phi(M) = \Phi(S = 3/2, M)$.

to the effective ZFS parameter $2D_{\text{eff}} = 2(D_0 - |D_{\text{DM}}'|)$ since the repulsion of the ground $|M| = 3/2$ doublet is $\sqrt{3}$ times larger than the repulsion of the ground $|M| = 1/2$ doublet: $E(3/2, |M| = 3/2) = -3|J_0|/2 - l_{\text{DM}} + D_0 - |D_{\text{DM}}'|$, $E(3/2, |M| = 1/2) = -3|J_0|/2 - l_{\text{DM}} - D_0 + |D_{\text{DM}}'|$. In the case if $D_0 < |D_{\text{DM}}'|$, the $|3/2, 3/2\rangle$ doublet is the ground state, $D_{\text{eff}} < 0$. The ZFS $2D_0$ has the anisotropic exchange origin.^{20a,21a,23a,34,35} For the FM Cu_3 cluster with the parameters (in cm^{-1}) $J_0 = -109$, $|G_{x,z}| = 40$, the DM ZFS contribution $2D_{\text{DM}}'$ depends significantly on the value and sign of the DM exchange parameters: $2D_{\text{DM}}' = -2.16 \text{ cm}^{-1}$ for $G_{x,z} = 40 \text{ cm}^{-1}$ and $2D_{\text{DM}}' = -5.14 \text{ cm}^{-1}$ for $G_{x,z} = -40 \text{ cm}^{-1}$. The dependence on the sign of G_z is opposite to that of the case of the excited $S = 3/2$ state of the AFM cluster (Figure 2). The DM(x) contribution $2D_{\text{DM}}'$ to ZFS of GS 4A_2 may be of the order of the experimentally observed^{21a} ZFS $2D_e = -5 \text{ cm}^{-1}$.

In the trigonal FM Cu_3 cluster²² with $J_0 = -1.52 \text{ cm}^{-1}$, an axial ZFS parameter $D_{3/2} = -74 \times 10^{-4} \text{ cm}^{-1}$ was found experimentally,²² which differs in sign and value from the possible spin-spin dipolar contribution ($D_{\text{dip},3/2} = +15 \times 10^{-4} \text{ cm}^{-1}$).²² In the case of the DM exchange parameter $G_z = 0.12|J_0|$ (as in ref 21a), the DM(x,y) contribution to the ZFS parameter is $D_{\text{DM},3/2} = -70 \times 10^{-4} \text{ cm}^{-1}$, which is of the order of $D_{3/2}$.

7. Conclusion

The mixing of the ground spin-frustrated $2(S = 1/2)$ and excited $S = 3/2$ states by the in-plane DM exchange results in the large positive DM exchange contribution $2D_{\text{DM}}$ to ZFS of the excited $S = 3/2$ state of the Cu_3 clusters with the strong DM exchange coupling. This $2D_{\text{DM}}$ contribution to ZFS

depends on the parameters G_x , G_z , and J . Since the chirality of the ground-state is determined by the sign of G_z , the dependence of the $S = 3/2$ ZFS on the sign of G_z shows the correlation between the chirality of the ground-state and ZFS $2D_{\text{DM}}$ of the excited $S = 3/2$. In the isosceles Cu_3 clusters, the in-plane DM exchange mixing results in the rhombic magnetic anisotropy of the $S = 3/2$ state, the nonlinear field dependence of the Zeeman levels of the $S = 3/2$ state in magnetic field $H = H_z$ and the field dependence of the intensities of the EPR transitions. Large δ -distortions result in the inequality ΔG_z of the pair DM parameters and the $S = 1/2$ - $S = 3/2$ mixing with $\Delta M = 0$ by the ΔG_z DM term, that leads to an additional magnetic anisotropy of the $S = 3/2$ state. In the AFM clusters, the in-plane DM exchange mixing (G_x , G_y) slightly influences the ZFS, magnetic anisotropy and EPR spectra of the ground $2(S = 1/2)$ states at low magnetic fields. In the ferromagnetic Cu_3 clusters, the in-plane DM exchange mixing of the ground $S = 3/2$ and excited $2(S = 1/2)$ states results in the large negative DM exchange contribution $2D_{\text{DM}}'$ to the axial ZFS $2D$ of the ground $S = 3/2$ state.

Appendix A

The energy matrix of the Hamiltonian (1) of the isosceles Cu_3 cluster with the account of the Heisenberg exchange, δ distortions, DM exchange, and axial ZFS has the form of Table A1.

Supporting Information Available: Equations S1–S9. This material is available free of charge via the Internet at <http://pubs.acs.org>.

IC701796Q